Available online at www.sciencedirect.com

ScienceDirect

Materials Today: Proceedings XX (2016) XXX–XXX

materialstoday: PROCEEDINGS

www.materialstoday.com/proceedings

PMME 2016

Experiment and predictions of strain and stress based failure limits for advanced high strength steel ☆

Chetan P Nikhare *

Mechanical Engineering, Penn State Behrend, Erie, PA – 16563, USA

Abstract

Strain based failure measurements are traditionally very popular and implemented to construct the failure limits. The predictions of these measurements through various models were compared and agreed for the conventional steels. Whereas continuous demand on the reduction of the vehicle mass while maintaining comfort and passenger safety for current and future vehicles car manufacturers are attracted to a newly developed advanced high strength steel. These steels that promises high strength and enhanced ductility were produce to reduce the impact of fuel usage by balancing the above demands. However while implementing these steels many challenges were faced by manufacturers and tool designers. One of the challenges is to predict the forming limit diagram through the conventional strain based models. In this paper experiments were performed on Dual Phase and Transformed Induced Plasticity steels to plot the forming limit diagram and further compared with the conventional strain based models. It was observed that strain based model under predicts the failure whereas stress based models are the best agreement with experiments.

Selection and Peer-review under responsibility of International Conference on Processing of Materials, Minerals and Energy (July 29th – 30th) 2016, Ongole, Andhra Pradesh, India.

Keywords: AHSS, forming limit diagram, strain based failure, stress based failure, numerical simulation

* Corresponding author. Tel.: +1-814-898-7588; fax: +1-814-898-6125.
E-mail address: cpn10@psu.edu

Selection and Peer-review under responsibility of International Conference on Processing of Materials, Minerals and Energy (July 29th – 30th) 2016, Ongole, Andhra Pradesh, India.

1. Introduction

Due to steep growth of environmental concern, strict regulations took step forward on vehicle fuel economy to increase to 41 mpg by 2016 and to as high as 61 mpg by 2025 as compared to the current status of 30.2 mpg CAFE (Corporate Average Fuel Economy) standard [1]. To cope with this demand one way is to switch to smaller vehicles and other way is to reduce the vehicle weight without compromising on price and safety for the customers. Advanced High Strength Steels (AHSS) are effective in thickness reduction of automotive parts without compromising the strength and crash performance and are therefore a promising solution if weight reduction in combination with increased safety is required [2].

Steels with 700MPa or greater ultimate tensile strength are AHSS as defined by ULSAB (Ultra-Light Steel Auto Body) [3]. These steels produce unique mechanical properties with generally having multiphase microstructure containing sufficient quantities of martensite, bainite and/or retained austenite. An excellent combination of high strength and high formability resulting primarily from their high strain hardening capabilities generally exhibits by these AHSS [4-8]. However some affecting factors limits the usage of these steel in many application due to lack of understanding of these material behavior during forming [9-10]. These steels can show large to unpredictable springback and sudden failure without any notification of necking [2, 9-11].

In 1966 Keeler [12] proposed a way to measure the tearing failure in sheet metal forming which is known as a strain based failure criterion. This strain based failure criterion is a plot of minor and major strain on the plane of the sheet during deformation which further called as Forming Limit Diagram (FLD). Goodwin [13] further demonstrated this method to analyze the sheet metal necking and failure by predicting the forming limits. This FLD includes a single curve (called as Forming Limit Curve; FLC) for a material from uniaxial to biaxial stretching by measuring and plotting strain just prior to failure. If the strain value at any given location on a material which is deforming along a particular strain path (strain path assumed to be linear) is above the FLC, then the material failed due to tearing and if the strain value is below the FLC then the material is safe and would not fail due to tearing.

Due to its nature the strain can be easily measured and quantified physically and thus is popularly used during die tryouts and in production of the formed parts and also in quality checks. Though it is easy to measure this parameter it is likely a good representation for the parts which go under various stamping stages as FLC is dependent on the strain path through which metal undergoes during deformation. This was demonstrated by plotting the FLC's for different prestrained material and observed that FLC shifts in strain space depending on the strain path applied both in pre-strained and post-strained [14-16]. Other concern which noted recently is that this failure criterion is unable to accurately plot the limit curve for material which can fail due to sudden fracture without any necking [17]. The typical failure mode observed over the time during stamping of some mild and conventional high strength steel is localized necking and eventually results in splitting of parts. This kind of necking and failure mode is very commonly related to the critical strain intensity in the part [11]. Previous forming research on Dual Phase (DP) steels noticed that conventional forming limit diagrams, FLDs are sufficient to describe the failure where localized necking occurs [18-20]. However, in some deformation modes like in bending fractures were not accurately predicted due to lack of necking which resulted in sudden failure. For such cases FLD curves does not provide the good estimation of fracture [10, 17, and 21]. Thus to correctly predict the estimation of fracture for these multiphase steels an alternative method is desired and which may be stress based failure criterion.

The first literature encountered on failure criterion stress based failure criterion was proposed by Arrieux et. al [15]. The stress based limit diagram was plotted for titanium material for linear strain paths, pre-strain stretching and pre-strain tension. It was also noted that this limit diagram is independent on strain paths. The strain based FLC which was plotted by Graf and Hosford [14] for different prestrained material was further analytically converted stress space by Stoughton [22] and observed that they converge to approximately a single curve. Though it is hard to physically measure the stress value during deformation of parts, but analytical or numerical methods can be used to predict the stress and further failure and these information can used to design the components. Previous studies were performed to predict failure using stress based failure criterion by performing the dome forming numerical simulations [23]. Using various yield criteria (von Mises, Hill '48, and Barlat '89) first the strain based FLD was analytically converted to stress based FLD. Further the strain path data from the numerical simulation of eight dome tests was analytically converted to stress paths and predicted the failure by analyzing stress values which falls above

the stress based FLD. Good correlation was found for all cases. Some of the experimental validation related to stress-based FLD was performed by Moondra and Kinsey [24].

In this paper two AHSS Dual Phase and Transformed Induced Plasticity steels were considered. The steel was bi-axially stretched and failure, dome depth and thickness distribution was analyzed. Further experimental strain based FLD were used and compared with the two conventional strain based models: M-K model and thickness gradient criterion. In addition the stress based failure criterion using von-Mises yield criterion was plotted and stress values from the model was compared.

2. Material and methodology

The two types of steels investigated in this study are DP and TRIP. Their individual measured thicknesses and chemical compositions are shown in the Table 1.

Table 1: Measured thickness and chemical composition ranges of DP and TRIP steels

Designation	Thickness (mm)	Chemical composition, %				
		C	Si	Mn	P	S
DP	1.97	0.15max	1.50max	2.00max	0.025max	0.010max
TRIP	2.04	0.21max	2.20max	1.80max	0.025max	0.010max

Australian standard AS 1391-1991 was used to create the tensile specimens and perform the tensile tests. The specimens were oriented along the rolling direction. A test range of 25±5mm was used with a non-contact extensometer. 30 kN MTS test machine was used to perform all tensile tests. On all specimens' flat gauge section two white dots were marked, placed 25 mm apart from each other. The displacement of the dots during testing was measured using a camera system. A strain rate of 2 mm/min was used to perform the test. The force displacement data was also captured [25].

The true stress-strain curves determined in the tensile test are shown in Figure 1. It can be seen that the TRIP steel exhibits lower initial work hardening compared to the DP steel, while the DP steel shows a lower UTS and minimum elongation compared to TRIP. Nevertheless, compared to previous studies involving the forming behavior of AHSS and conventional steel grades, the steels investigated in this work show very similar tensile properties.

The stress strain curves of all three steel types were fitted using a power law (equation 1).

$$\sigma = K\varepsilon^{n} \quad (1)$$

where, σ = True stress; ε = True strain; K = Strength coefficient; n = Strain hardening exponent

The fitted power laws did not provide a good representation of near yield behavior. This difference is because the strain hardening exponent was determined by using the later tensile region of 10% strain [25]. Figure 1 shows the experimental true stress-strain curves with dotted extension with the power laws. This mix curves were used for simulation purposes.

2.1. Erichsen stretch forming

The Erichsen sheet metal tester was used to perform the stretch forming tests for the biaxial strain condition. The tooling for stretch forming is shown in Figure 2. The radius for the lock-bead was 5mm. For lubrication purpose, a sandwich of polymer foil (thickness of thin foil = 0.1mm and thick foil = 0.35mm) together with oil was used in each test. The blank holding force of 230 kN and the punch speed of 100 mm/min were used during the test. Some of the tests were stopped at a final punch stroke 22mm (approximately five and half millimeters before the initiation of necking observed for DP) to measure the thickness distribution while others were performed until failure of the sheet. Note that an initial test speed of 100mm/min was used however for the exact determination of the initiation of necking the test speed was reduced towards the end [26].

2.2. Thickness measurement

To measure the thickness of the formed hemispherical cup, a small strip of the test specimen was cut from the center along the rolling direction. The center region of span of 24mm where the thickness measurements were taken. Marks were indented using a Vickers's hardness tester along the specimen edge in a pre-defined distance of 2 mm [25]. These indentations were the reference point of the particular section where the thickness was desired. At those indented points the images were captured with the help of an optical microscope. With a proper magnification generally at least two indentations were able to frame in each image. Further with the help of Image tool (version 3) software [27], the thicknesses were measured at each of those indented points.

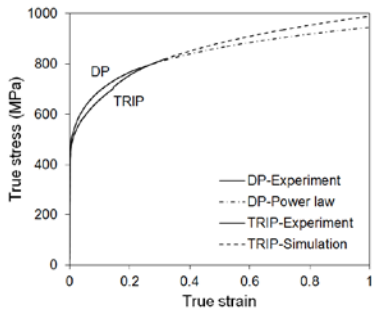

Fig. 1. True stress-strain curves determined in the tensile tests plus power law for DP and TRIP steels

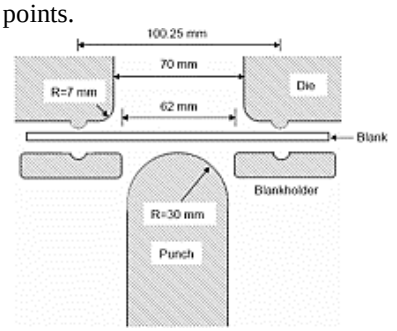

Fig. 2. Erichsen stretch forming experimental set-up

2.3. Numerical approach

The Erichsen sheet metal stretch forming test was modeled using ABAQUS/Explicit 6.5-1. A three-dimensional model approach was taken to simulate the stretch forming. Rigid surfaces was applied to the tooling. To mesh the deformable blank M3D4R membrane elements (4-node quadrilateral, reduced integration) were used. Full model was used to reduce any discrepancy for both tests. The material properties were inputted as a tensile true stress-strain curve in the model which was determined during the experimental tensile test. Isotropic hardening option in the model was applied. The sheet thickness as detailed in Table 1 was applied to the respective sheet in the respective model [26].

As observed previously that the fitted power law could not able to match well with the earlier part of the experimental tensile curve. Thus the material input data for the model was set such that a combination of both data was applied. The earlier part of the curve i.e. less than 10% strain the experimental test data was used and fitted power law was used to generate the later part of the curve i.e., above 10% of strain data [26].

The model was equipped and detailed with the same process parameters as applied in experiments. The interaction between the blank and the rigid bodies was assumed zero friction as in experiments the process was highly lubricated (grease and thin and thick polyethylene foils). Due to the assumption of no material sliding through the lock bead during deformation the flange part was ignored for simulation purpose. Thus the boundary conditions was applied such that the outside edge (section where the lock-bead indents the sheet) of the sheet metal kept fixed. This boundary condition is valid with the assumption that a perfect clamping is occurred and no sliding of metal would take place during deformation between the blankholder and the die surface [26].

In the stretch forming tests the TRIP steel showed the highest formability compared to DP (Figure 3). While the DP could only be formed to a maximum cup height of 27.5mm, the maximum cup heights achieved for TRIP steel was 31mm, respectively.

The force displacement curves numerically predicted for the stretch forming process are compared to the experimental data in Figure 3. Good correlation between the experimental results and the FEA predictions is achieved for both steels.

The thickness distribution over the span of 24mm from the apex of the cup for both steels is shown in Figure 7. The DP steel undergoes higher thinning than the TRIP steel. The FEA prediction gives very good agreement with the experiments (Figure 4).

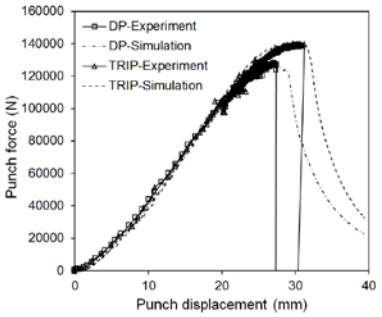

Fig. 3. Experimental and numerical force-displacement curve for DP and TRIP steel

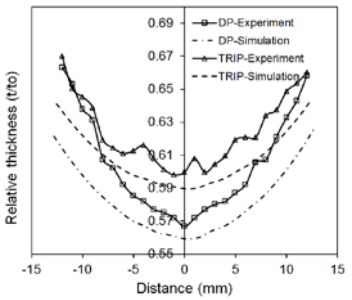

Fig. 4. Experimental and numerical thickness distribution for DP and TRIP steel at 22 mm punch depth

3. Strain based forming limit diagram

3.1. Experiments

To generate the whole range of limit strains from uniaxial to biaxial strain the Erichsen sheet metal tester with the stretch forming tool was used. Strips with a length of 150mm and various widths between 5 to 150mm were used to produce different deformation paths. Circle grids having a diameter of 2.5mm were electrochemically etched on the specimens for strain measurements. For lubrication purpose a sandwich construction of oil together with two PP-foils was used for each test. For each test trial, the specimens were clamped on their edges with a blankholder force of 230kN and stretched by the hemispherical punch until necking occurred. During the test the punch moves with the velocity of 100mm/min, while towards the end of each test the velocity was decreased so as to allow easy determination of the onset of necking. Using the grid analyser GPA 3.0, the deformation of circles was evaluated and the FLD was obtained by plotting the line between the strains for the necked and the safe points.

3.2. Predictions

Numerical simulations were performed using stretch forming model for all specimens from the range of uniaxial to biaxial mode of deformation. The forming limit was predicted using two criteria: M-K model and Thickness gradient criterion.

M-K model: The M-K analysis assumes that an initial defect in the sheet, in the form of a long groove, grows and eventually fails during stretching along the linear strain path in surrounding material. The pre-existing defect lies perpendicular to the major axis. This two zone material is subjected to plastic deformation applying a constant incremental stretching of the homogeneous part. When the flow localization occurs in the groove at a critical strain in the homogeneous region, the limiting strain of the sheet is reached. Then, the values of the major and the minor strain increments in the homogeneous region are reported for numerical plotting of forming limit diagrams [17].

$$\Delta\varepsilon_{a1}<0.1\Delta\varepsilon_{b1} \quad (2)$$

Thickness gradient criterion (TGC): With the application of load the metal undergoes deformation and perceives necking region as soon as the load equivalent to the tensile stress is applied. The perception of neck occurs with the occurrence of thinning in the metal. This localized necking occurs and flows rapidly with slight increase in force or stress is due to local critical thickness gradient perceives. This occurrence of neck is found to be independent of the deformation path, speed of forming and type of the sheet metal (i.e. the material properties) which is being formed. The mentioned local critical thickness gradient R_{cri}, exists at the onset of a visible local neck. As soon as the deformation starts a thickness gradient, "$R_{thickness\ gradient}$" develops in the sheet which is being deformed and is expressed as

$$R_{thickness\ gradient} = \frac{Current\ thickness\ of\ neck\ element}{Current\ thickness\ of\ neighbour\ element} \quad (3)$$

This thickness gradient reduces due to continuation of deformation and decreases from the initial value of 1.0. At the onset of localized necking this thickness gradient becomes steeper and at the transition from diffused neck it attains a critical value [26]. This criterion is represented by

$$R_{thickness\ gradient} \leq R_{cri} \quad (4)$$

R_{cri} has been experimentally estimated as 0.92 [28-29]. Also at the point that this criterion was met the cup depth at neck was measured.

Using M-K model and TGC the strain based limit strains were predicted and plotted for both DP and TRIP steel in all strain direction and is shown in Figure 5 and 6. It can be observed that both models predict the similar forming limit strains to each other. However they did not provide the good agreement with the experimental results. Both model under predicts the forming limit strain as compared to experiments. It is also observed that the maximum difference error in match with the experiment is in plane strain. However it decreases towards uniaxial or biaxial direction. The prediction in forming limit strain is poor is due to lack of information provided to the numerical material model. For conventional steels the continuum material model would provide the good agreement with the experiment however due to multi-phase structure of these advanced high strength steels more sophisticated multi-scale modeling would be necessary to compare the behavior. Due to differences in the properties of each phase the interaction between phases are important. It was found that due to the strength difference in the phases, the deformation mechanism provides different failure behavior [11]. As conventional numerical models are best fit with the conventional steel, they provide inaccurate results for more advanced materials like AHSS and thus provide premature failure. Hence upon using the numerical simulation will only provide the inaccurate guesses on formability for these advanced materials and end up with over design of dies.

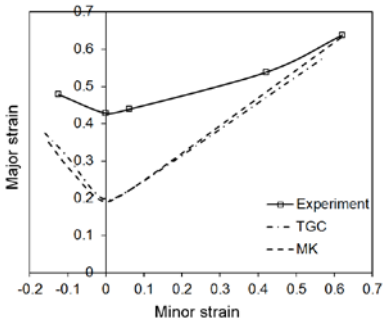

Fig. 5. Strain based forming limit diagram for DP steel

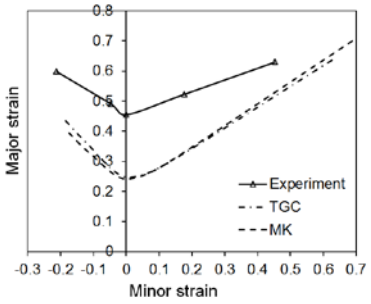

Fig. 6. Strain based forming limit diagram for TRIP steel

4. Stress based failure criterion

In order to obtain plots of the stress path, the strain path data was analytically converted using the von-Mises yield criterion and is given in [23]. Using the stress based failure criterion the strain data from experiments and from both models which were plotted as forming limit curve in figure 5 and 6 were analytically converted to a stress space and plotted as shown in Figure 7 and 8. The forming limits on the stress space from both models still under predict the experiment limit strains. This is because the stress limits were directly converted from the strain data as presented in Figure 5 and 6. However these strain values are lesser than experiments and thus direct conversion will provide less stress value. It means if the material is more stretched by increasing the dome depth until it reaches above the experimental stress FLC the material is assumed to be safe and with these stress limits the failure guesses will be accurate and optimized die design could happen.

5. Conclusion

From the tensile tests it was shown that the two steel types investigated in this study had similar tensile properties suggesting a comparable forming behavior. However, in the stretch forming tests higher thinning was observed in the DP steel compared to the TRIP steel. Further the necking occurred for DP steel was at lesser punch depth than

compared to TRIP steel. Experimental forming limit curve was plotted and compared with the predicted values from M-K model and TGC. However it was observed that strain based forming limit models under predicted the failure whereas stress based provides the closer agreement. Thus it is concluded that the stress based failure criterion would be better to predict the forming limit values for advanced high strength steels.

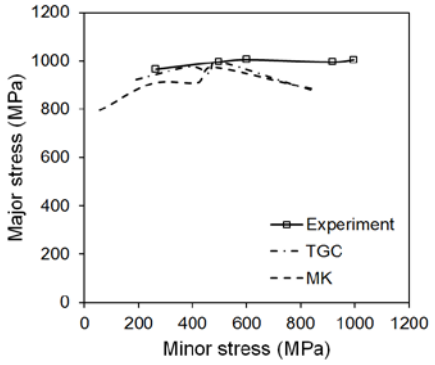

Fig. 7. Stress based forming limit diagram for DP steel

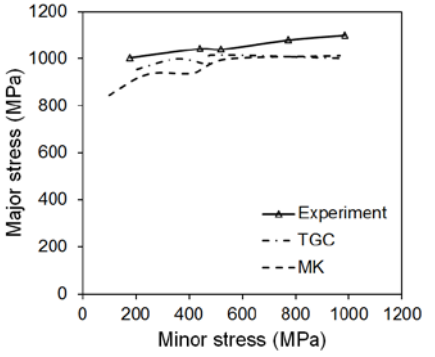

Fig. 8. Stress based forming limit diagram for TRIP steel

Acknowledgements

The author would like to thank Prof. Brad Kinsey and Prof. Yannis Korkolis for the support and lab facility provided at University of New Hampshire during this research.

References

[1] National Highway Traffic Safety Administration. 2017-2025 Model Year Light-Duty Vehicle GHG Emissions and CAFE Standards: Supplemental 2011.
[2] Y. Mukai, Kobelco Technology Review no. 26 (2005).
[3] International Iron and Steel Institute: www.worldautosteel.org.
[4] C.D. Horvath, J.R. Fekete, International Symposium on Advanced High Strength Steels for Automotive Applications, The Minerals, Metals and Material Society (TMS) (2004) 107–115.
[5] A. Satorres, Master's Thesis, University of Oulu (2005).
[6] H.K.D.H. Bhadeshia, ISIJ International 42 (2002) 1059-1060.
[7] J.R. Fekete, Int. Symp. On Niobium Microalloyed Sheet Steel for Automotive Applications, The Minerals, Metals and Material Society (TMS). (2005) 107-115.
[8] C. Nikhare, Performance behaviour of AHSS. learningspaces.edu.au
[9] R.H. Wagoner, G.R. Smith, The Ohio State University (2006).
[10] J.R. Fekete, Processing, Microstructure, Properties and Peformance (2007) 1-9.
[11] C. Nikhare, P.D. Hodgson, M. Weiss, Materials Science and Engineering A 528 (2001) 3010-3013.
[12] S.P. Keeler, Trans SAE, 74, paper no. 650355 (1966).
[13] G.M. Goodwin, SAE paper No. 680093 (1968).
[14] A. Graf, and W. Hosford, Metallurgical Transactions 24A (1993) 2503-2512.
[15] R. Arrieux, Annals of CIRP 36 (1987) 195-198.
[16] R. Arrieux, C. Bedrin, M. Boivin, 12th IDDRG Congress, Santa Margherita Ligure. 2 (1982) 61-71.
[17] W.F. Hosford, R.M. Caddell, Metal Forming- Mechanics and Metallurgy. Second Edition, Prentice Hall (1993).
[18] A.A. Konieczny, International Body Engineering Conference (IBEC), SAE Technical Paper No. 2001-01-3106 (2001).
[19] S. Sriram, B. Yan, M. Huang, SAE Technical Paper No. 2004-01-0506. (2004).
[20] M.F. Shi, S. Gelisse, IDDRG. (2006) 19-26.
[21] International Iron and Steel Institute, www.worldautosteel.org, (2005).
[22] T.B. Stoughton, Journal of Engineering Materials and Technology 123 (2001) 417-422.
[23] A. Sakash, S. Moondra, and B. Kinsey, Journal of Engineering Materials and Technology 128 (2006) 436-444.
[24] S. Moondra, and B. Kinsey, Transactions of the North American Manufacturing Research Institute of SME 32 (2004) 247-254.
[25] C. Nikhare, M. Weiss, and P.D. Hodgson, In Metal Forming 2008 : Proceedings of the 12th International Conference on Metal Forming. (2008) 272-279.
[26] C. Nikhare, A. Asgari, M. Weiss, and P.D. Hodgson, Steel Research International 81 (2010) 1450-1453.
[27] http://ddsdx.uthscsa.edu/dig/itdesc.html
[28] S. Kumar, P.P. Date, K. Narasimhan, Journal of Materials Processing Technology 45 (1994) 583-588.
[29] V. Nandedkar, PhD Thesis IIT-Bombay (2000).